

Comparison of three effective Hamiltonian models of increasing complexity: Triazene in water as a test case

I. Fdez. Galván, M. E. Martín, and M. A. Aguilar^{a)}

Departamento de Química Física, Facultad de Ciencias, Universidad de Extremadura, Avenida de Elvas s/n, 06071 Badajoz, Spain

M. F. Ruiz-López

Équipe de Chimie et Biochimie Théoriques, UMR CNRS-UHP No 7565, Université Henri Poincaré, B.P. 239, 54506 Vandœuvre-lès-Nancy, France

(Received 29 December 2005; accepted 3 April 2006; published online 5 June 2006)

A critical comparison of widely used solvation models is reported. It is illustrated by a study of the triazene molecule in liquid water. We consider the following approaches: (1) a continuum model based on multicentric multipole expansions of the charge distribution, (2) the averaged solvent electrostatic potential from molecular dynamics (ASEP/MD) method, and (3) molecular dynamics simulations using a combined quantum mechanics/molecular mechanics potential (QM/MM/MD). We find that the solvation induces appreciable changes in the geometry and charge distribution of triazene. These changes are only qualitatively reproduced by the dielectric continuum model, which clearly underestimates induced dipole moments and solute-solvent interaction energy. We also show that the use of effective point charges placed on solute nuclei during the classical simulations may cause significant errors in the description of the solvent structure. The addition of charges representing nitrogen atom lone pairs is compulsory to reproduce the QM/MM/MD simulation results. Moreover, our results validate the use of the mean field approximation in the study of solvent effects. A major conclusion of this study is that the ASEP/MD method constitutes a reliable alternative to the much more computationally demanding QM/MM/MD methods. © 2006 American Institute of Physics. [DOI: 10.1063/1.2199528]

INTRODUCTION

Because of their high precision to economy ratio, the effective Hamiltonian (EH) methods¹ have been widely employed in the study of liquids and solutions. In EH methods, the solute is described quantum mechanically while the solvent effect is included as a perturbation in the solute molecular Hamiltonian. The most used technique in this context is certainly the continuum model but many efforts have been devoted to the development of more elaborated approaches that consider explicit solvent molecules and combine quantum computations with statistical mechanics. A general and critical comparison of available approaches is still lacking though it would be of main interest for a wide community of researchers developing models or working in the field of computational chemistry and biochemistry.

In this paper, we have carried out such a comparison for three EH methods that represent three levels of increasing complexity and, therefore, of computational cost. Specifically, we consider, (1) a continuum model based on the use of a multicenter multipolar expansion (MPE) of the charge distribution,^{2–6} (2) the averaged solvent electrostatic potential from molecular dynamics data (ASEP/MD) method,^{7–11} (3) and molecular dynamics simulations using a combined quantum mechanics/molecular mechanics potential (QM/MM/MD).^{12–15}

The three methods differ in the description of the solvent

perturbation. MPE and ASEP/MD make use of the mean field approximation¹⁶ (MFA), which assumes that the solute structure can be obtained from a quantum mechanical calculation carried out in the presence of the average perturbation produced by the solvent. The MPE method neglects the microscopic structure of the solvent, which instead is represented as a dielectric continuum, and involves a single quantum mechanical calculation. In the ASEP/MD method, the solvent microscopic structure is accounted for by carrying out classical molecular dynamics simulations. In general, it involves a fast-convergent iterative procedure in which the solute charges used in the classical MD simulation are updated from a quantum mechanical calculation in the ASEP. In contrast to the MPE and ASEP/MD methods, the MFA is not used in the QM/MM/MD approach. Rather, the solute properties are obtained as a time average from the simulation. A quantum mechanical computation is done at each step of the simulation for the solute interacting with the solvent charges.

Obviously, the main advantage of the MFA is that it permits one to reduce the number of quantum mechanical calculations from the several thousands that are necessary in a QM/MM simulation to only one (MPE) or a few (ASEP/MD). The price to pay is the neglect of the role played by instantaneous polarization. In particular, one disregards the Stark contribution¹⁶ to both the solvation energy and the solvent structure. By comparing the results obtained with the three methods, we set out to determine the validity of the

^{a)}Electronic mail: maguilar@unex.es

MFA and the importance that explicit consideration of the solvent structure has on the MFA results for the solute properties.

An additional question that we address concerns the choice of a point charge distribution in classical simulations. As explained below, the ASEP/MD method uses a dual representation of the solute charge distribution. At each cycle of the ASEP/MD calculation, the solute charge distribution is updated using quantum mechanics but during the molecular dynamics simulations the solute charge distribution is represented by a set of fixed point charges. This dual character in the solute representation can introduce errors in the estimation of the solvent structure, and hence of the solute's properties.

In a very interesting paper, Takahashi *et al.*¹⁷ showed that the atomic point charge representation as well as the MFA, i.e., the use of a fixed electron distribution during the MD simulation, is able to reproduce the results of the QM/MM simulation for the water molecule in liquid water. We had reached the same conclusion in a previous paper.¹⁸ However, Takahashi *et al.*¹⁷ also found that the use of an atomic point charge representation gives incorrect results when it is applied to anionic systems. In this paper we compare the performance of several point charge distributions, and show how the use of additional charges representing the free electron pairs notably improves the results. Obviously, the conclusions are applicable not only to ASEP/MD but to all classical simulations where the molecules are represented through point charge sets.

As a test case, we chose triazene in aqueous solution. Triazenes are chemicals characterized by the presence of a diazoamine group. The stability, equilibrium, and decomposition of substituted triazenes have been studied experimentally¹⁹⁻²⁵ and theoretically.²⁶⁻³⁰ The simplest member of the family is known as triazene $\text{HN}=\text{NNH}_2$. The solvation of this compound is interesting because each of its three nitrogen atoms has a different chemical environment and hence interacts with the solvent in a different way. Furthermore, the molecule is quite flexible, and appears to be a severe test for theories using the MFA.

METHODS

The three methods used in this paper belong to the group of the so-called effective Hamiltonian methods,¹ where the solute structure is obtained in the presence of the perturbation originated by the solvent

$$(\hat{H}^0 + V_{\text{int}})\Psi = E\Psi. \quad (1)$$

Here, \hat{H}^0 is the gas phase Hamiltonian, the operator V_{int} accounts for the perturbation due to the solvent, and Ψ is the solute wave function in solution. Differences between the methods are due to different descriptions of V_{int} . The main characteristics of the methods are outlined below. The interested reader should refer to the original papers for further details.

MPE CONTINUUM MODEL

The continuum model that we use is a self-consistent reaction field (SCRf) method developed at Nancy²⁻⁶ and based on a truncated multicenter multipole expansion. In this model the solute is inside a cavity adapted to the molecular shape and surrounded by a dielectric characterized by a dielectric constant, ϵ . The interaction potential takes the form

$$V_{\text{int}} = \sum_{I,j} \sum_l \sum_{m=-l}^l M_l^m(I) R_l^m(I,J), \quad (2)$$

where $M_l^m(I)$ are the multipole moment components at center I of the solute charge distribution and $R_l^m(I,J)$ are the components of the reaction field depending on centers I and J .

ASEP MOLECULAR DYNAMICS

In the ASEP/MD method,⁷⁻¹¹ one uses the MFA to compute the solute's wavefunction. The electrostatic interaction term is now evaluated from the equation

$$\hat{H}_{\text{QM/MM}}^{\text{elect}} = \int dr \cdot \rho \cdot V_s(r), \quad (3)$$

where ρ is the solute charge distribution, and V_s is the averaged solvent electrostatic potential or ASEP:

$$V_s(r) = \langle \hat{V}_s(r,X) \rangle. \quad (4)$$

The angle brackets indicate a statistical average over the solvent configurations. In practice, one must perform a complete MD simulation using a classical force field followed by a computation of the corresponding ASEP and a quantum calculation for the solute molecule interacting with the ASEP. An iterative procedure is carried out in which the solute charges in the MD simulation are taken from the preceding quantum computation. Convergence is reached quite rapidly, even when the initial solute charges are those obtained in the gas phase (about 5–15 cycles). The final results are obtained by averaging the values of the last converged cycles.

QM/MM MOLECULAR DYNAMICS

The Hamiltonian of the solute-solvent system contains three terms:

$$\hat{H} = \hat{H}_{\text{QM}} + \hat{H}_{\text{MM}} + \hat{H}_{\text{QM/MM}}, \quad (5)$$

where \hat{H}_{QM} contains the interactions in the quantum subsystem (the solute) with nuclei and electrons explicitly represented, \hat{H}_{MM} contains the interactions in the classical subsystem (the solvent), and $\hat{H}_{\text{QM/MM}}$ contains the QM/MM interactions and corresponds to the V_{int} term of Eq. (1).

For a specific point of the configurational space, the energy and wave function of the solvated solute molecule are obtained by solving the effective Schrödinger equation (1) where the interaction term now takes the form

$$V_{\text{int}} = H_{\text{QM/MM}}^{\text{elect}} + H_{\text{QM/MM}}^{\text{vdw}}. \quad (6)$$

TABLE I. Computed solute-solvent interaction energies (in kcal/mol), geometry (in angstrom and degrees) and dipole moment (in debyes) of triazene *in vacuo* and aqueous solution using different effective Hamiltonian methods.

| | <i>In vacuo</i> | SCRF | Semicontinuum ^a | ASEP/MD set 6 | DFMM |
|------------------|-----------------|-------|----------------------------|------------------|-------------|
| N1=N2 | 1.271 | 1.276 | 1.281 | 1.287 | 1.283±0.031 |
| N2-N3 | 1.354 | 1.342 | 1.318 | 1.321 | 1.331±0.030 |
| N1-H4 | 1.035 | 1.033 | 1.038 | 1.039 | 1.047±0.026 |
| N3-H5 | 1.016 | 1.017 | 1.032 | 1.021 | 1.044±0.027 |
| N3-H6 | 1.028 | 1.027 | 1.048 | 1.030 | 1.049±0.028 |
| N1=N2-N3 | 112.6 | 113.8 | 118.7 | 114.4 | 115.5±2.7 |
| N2=N1-H4 | 104.8 | 105.0 | 104.7 | 105.6 | 105.9±3.6 |
| N2-N3-H5 | 113.3 | 114.3 | 112.3 | 116.6 | 114.8±4.1 |
| N2-N3-H6 | 116.8 | 118.3 | 122.6 | 122.1 | 119.9±4.3 |
| N1=N2-N3-H5 | 159.0 | 161.1 | 173.8 | 179.0 | 178.8±15.9 |
| N1=N2-N3-H6 | 16.2 | 15.8 | 5.6 | 0.9 | -1.1±15.7 |
| μ | 1.70 | 2.39 | | 3.08 | 3.19±0.41 |
| E_{int} | ... | -13.7 | | -24.9±0.4 | -36.8±2.5 |

^aTriazene +5 water molecules inside a dielectric.

$H_{\text{QM/MM}}^{\text{elect}}$ contains the electrostatic terms and $H_{\text{QM/MM}}^{\text{vdw}}$ the van der Waals interactions, in general described by a Lennard-Jones potential.

In the DFT/MM/MD method developed at Nancy,¹²⁻¹⁵ the solute wave function is computed at each step of the MD simulation using density functional theory and Eq. (1). The forces acting on nuclei (QM and MM) are evaluated, and the equations of motion are solved to obtain the new atom positions. Average energies and properties are computed at the end of the QM/MM/MD simulation.

TECHNICAL DETAILS

The QM molecular wave function was obtained at the density functional theory (DFT) level using the BP86 (Ref. 31) functional. The basis set quality was N(7111/411/1)H(41/1).³² The DEMON³³ and GAUSSIAN³⁴ programs were used to perform the DFT calculations in the DFT/MM/MD and ASEP/MD simulations, respectively. The simulations were carried out using the programs DFMM (Refs. 12-15) (for DFT/MM/MD) and MOLDY³⁵ (for ASEP/MD). The continuum calculations were performed using a version of the SCRF MPE model implemented in GAUSSIAN 03.^{5,6} The multipole expansion on each solute atomic center was truncated at $l=4$ and the continuum was characterized by a relative permittivity of 78.39. Note that calculations using the standard PCM model implemented in GAUSSIAN03 lead to results very close to those obtained with MPE provided one uses the same solute cavity.³⁶ In our case, the cavity is adapted to the molecular shape of the solute and is formed by a set of intersecting spheres with Bondi radii scaled by a factor of 1.2, the default value in GAUSSIAN03 and often used in the literature. The choice of the cavity may be crucial in continuum models. Some discussion of this point is given by Chalmet and Ruiz-López in comparing continuum calculations and QM/MM/MD simulations for the water molecule in liquid water.³⁷

The solute geometry was optimized in gas phase and solution with the MPE and ASEP/MD methods. In the

ASEP/MD case, we performed a complete optimization at each cycle of the procedure, using the rational function optimization (RFO) method.³⁸

In the ASEP and DFT/MM/MD simulations, the solute-solvent system consisted of 215 TIP3P (Ref. 39) water molecules and one DFT triazene molecule. The triazene-water Lennard-Jones potential parameters were taken from Ref. 40. A cubic simulation box of 18.7 Å was applied. Periodic boundary conditions and an appropriate cutoff (9.0 Å) were assumed.

In ASEP/MD, a time step of 0.5 fs was used. The electrostatic interaction was calculated with the Ewald method, and the temperature was fixed at 298 K by using a Nosé-Hoover⁴¹ thermostat. Each classical MD calculation simulation was run for 150 000 time steps (50 000 equilibration, 100 000 production) for each cycle. The final results were obtained as the average of the last five cycles. Initially, the charges used in the MD simulation were placed on the nuclei of the solute molecule. Since there is a total number of six charge centers, this set will be named set 6.

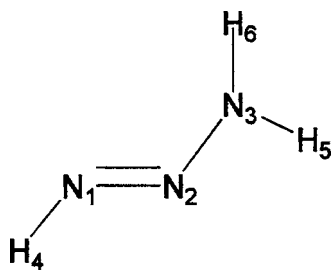
In the DFT/MM/MD calculations, the initial system configuration was chosen from the ASEP/MD results and, as a consequence, equilibration of the system required a very short simulation time. The production phase lasted 20 ps. The time step was 0.2 fs. Hydrogen nuclei were substituted by deuterium in order to reduce the vibrational frequency values.

RESULTS AND DISCUSSION

Solvent effects on solute structure

The computed geometry and dipole moment of triazene in aqueous solution are listed in Table I. For comparison, the geometry and dipole moment *in vacuo* are also given. Atom numbering is defined in scheme 1.

According to the most elaborate model used here, DFT/MM/MD, solvation increases the length of the N=N double bond, but decreases the length of the N-N single bond. These



SCHEME 1. Triazene molecule.

trends were reproduced by MPE and ASEP/MD, the latter method leading to results closer to the DFT/MM/MD ones. The largest discrepancies between the three methods appeared in the N–H distances. Due to hydrogen bond interactions with water, both DFT/MM/MD and ASEP/MD predict an increase of all N–H bond lengths while SCRF led to a small decrease in the case of N1–H4 and N3–H6. The magnitude of the NH bond length increase obtained in the DFT/MM/MD calculations is much larger than that predicted by ASEP/MD. For instance, for the N3–H5 bond, the solvent effect amounts to 0.028 and 0.005 Å, respectively. Another important difference between the approaches concerns the N1=N2–N3–H5 and N1=N2–N3–H6 torsion angles. *In vacuo*, the H5 and H6 atoms are out of the N1N2N3 plane. In other words, the N3 atom is slightly pyramidalized. In solution, the MPE method predicts a similar structure. However, the ASEP/MD and DFT/MM/MD methods predict an almost planar structure for the molecule. It may be interesting to note that the DFT/MM/MD simulation predicts high flexibility for the two torsion angle values, as shown in Fig. 1 which displays the corresponding statistical distribution. The most probable structure is flat, although the angles can reach values close to 50°. Further calculations with the continuum model in which the molecular geometry is constrained to be planar gave two interesting results. First, the energy of the optimized planar geometry is very close to that of the fully optimized triazene ($\Delta E=0.2$ kcal/mol). Second, in spite of their energy similarity, the two structures exhibit substantial bond length differences. Thus, for the planar triazene, MPE predicts the N1=N2 and N2–N3 bond distances to be 1.281 and 1.328 Å, which are not far from the DFT/MM/MD values. In order to further analyze the origin of the

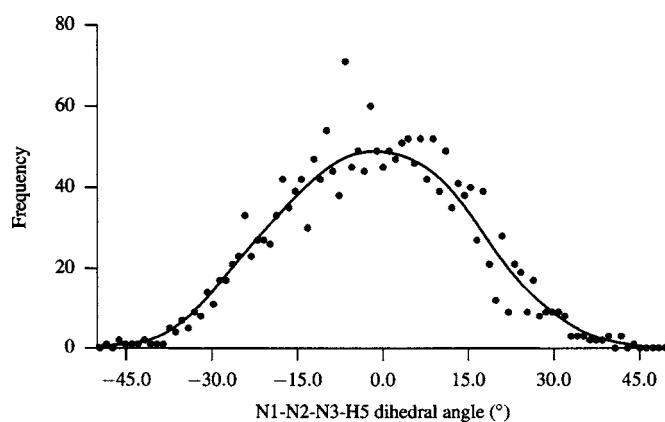


FIG. 1. Statistical distribution of N1=N2–N3–H5 torsion angles.

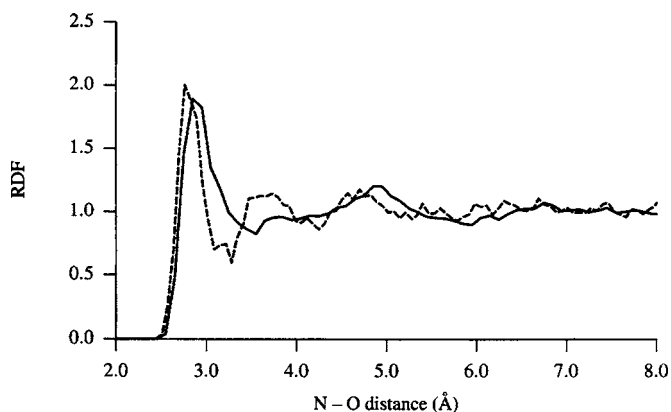


FIG. 2. Comparison between the nitrogen-1 (triazene)-oxygen (water) radial distribution functions obtained with DFMM (dashed line) and ASEP/MD, set 6 (full line).

differences between continuum and discrete solvation models, we performed additional calculations using a supermolecule-continuum method. We optimized a supermolecule composed of the triazene and five water molecules inside a dielectric continuum. The results are included in Table I. Indeed, explicit treatment of the first solvation shell appears to be fundamental since it considerably modifies the geometry obtained in the pure continuum approach. In particular, an almost planar structure is now predicted in good agreement with the ASEP/MD and DFT/MM/MD simulations. The N–N and N–H distances are also closer to the results obtained in the DFT/MM/MD simulations.

The changes induced by the solvent in the solute geometry, namely, the transition from a pyramidal to a planar structure of the molecule and the variations in the N–N distances, are consistent with a greater participation of a formal zwitterionic arrangement in solution: $\text{HN}=\text{N}-\text{NH}_2 \leftrightarrow \text{HN}^- - \text{N}=\text{N}^+\text{H}_2$. The stabilization of such a structure has an influence on the triazene charge distribution that is illustrated by the dipole moments in Table I. Solvation, as calculated at the DFT/MM/MD level, increases the dipole moment by about 88%. ASEP/MD and MPE also predict a substantial dipole moment increase. Analysis of the atomic charges shows that the positive charge increases on the N3 portion of the molecule, while the negative charge increases on the N1 portion.

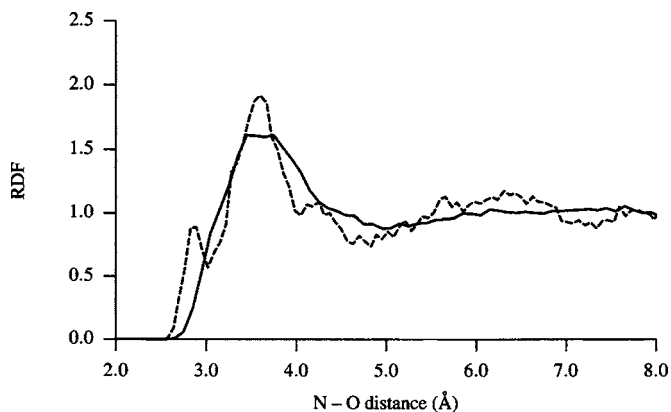


FIG. 3. Comparison between the nitrogen-2 (triazene)-oxygen (water) radial distribution functions obtained with DFMM (dashed line) and ASEP/MD, set 6 (full line).

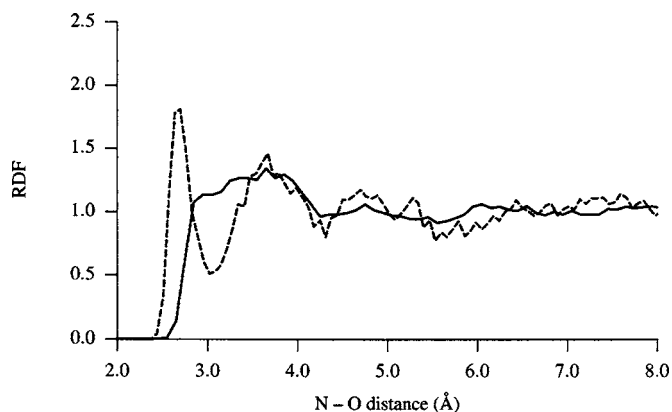


FIG. 4. Comparison between the nitrogen-3 (triazene)-oxygen (water) radial distribution functions obtained with DFMM (dashed line) and ASEP/MD, set 6 (full line).

Radial distribution functions

Let us now consider the solvent structure around the triazene molecule. Figures 2–4 display the radial distribution functions (rdf) between the triazene nitrogen atoms N1, N2 and N3 and the water oxygen atom, respectively.

When calculated with the DFT/MM/MD method, the N1–O rdf displays a well defined peak at 2.9 Å, characteristic of a hydrogen bond. There are also well-defined peaks, though less intense, at 3.7 and 4.8 Å. N3–O has a similar behavior, although compared to N1–O the first peak appears at a somewhat shorter distance, and the second peak is much more marked. N2–O displays a small peak at 2.8 Å and a secondary broad peak at 3.6 Å that can probably be associated with the first shell of N1 and N3. The integration of the first peak of the N1–O, N2–O, and N3–O rdfs up to the first minimum results in coordination numbers of 2.28, 0.81, and 1.83, respectively. N1 and N3 are involved in the formation of approximately two hydrogen bonds, while N2 is involved in only one hydrogen bond with water.

The ASEP/MD method yields a similar rdf for N1–O, although the first peak is slightly shifted towards a greater N–O distance, and the second peak is very small. Nevertheless, ASEP/MD completely fails to reproduce the solvent structure around N2 and N3. There are several reasons that may explain this shortcoming.

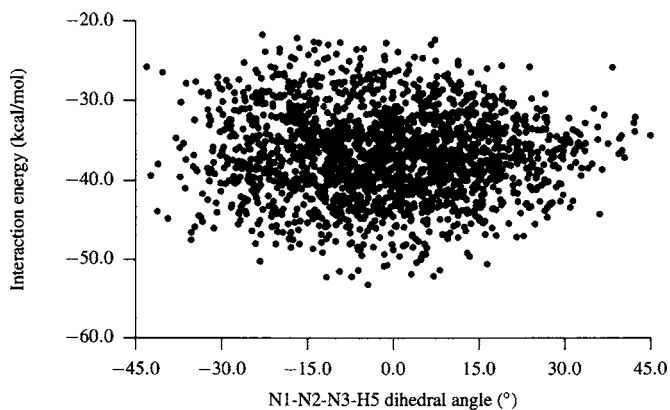


FIG. 5. Variation of the solute-solvent interaction energy with the N1=N2–N3–H5 torsion angle.

TABLE II. Computed solute-solvent interaction energies (in kcal/mol), geometry (in angstrom and degrees), and dipole moment (in debyes) of triazene molecule in aqueous solution using the ASEP/MD method and different point charge sets.

| | ASEP/MD set 9 | ASEP/MD set 10 |
|------------------|------------------|-------------------|
| N1=N2 | 1.278 | 1.277 |
| N2=N3 | 1.316 | 1.317 |
| N1-H4 | 1.035 | 1.038 |
| N3-H5 | 1.031 | 1.027 |
| N3-H6 | 1.037 | 1.035 |
| N1=N2–N3 | 116.9 | 117.1 |
| N2=N1–H4 | 106.3 | 106.5 |
| N2–N3–H5 | 115.7 | 115.8 |
| N2–N3–H6 | 122.5 | 122.5 |
| N1=N2–N3–H5 | 177.2 | 179.0 |
| N1=N2–N3–H6 | 2.6 | 1.1 |
| μ | 3.36 | 3.26 |
| E_{int} | -34.2 ± 0.8 | -33.3 ± 0.5 |

In principle, the ASEP/MD method differs from the DFT/MM/MD calculation in the following points:

- (1) ASEP/MD makes use of the mean field approximation, and hence does not account for the instantaneous charge fluctuations of the solute molecule, i.e., it neglects the influence of the Stark component on the energy and solvent structure.
- (2) ASEP/MD assumes the solute molecule to be rigid during the classical simulation, while the DFT/MM/MD method considers it to be flexible.
- (3) ASEP/MD describes the molecules classically during the simulation step, whereas in the DFT/MM/MD method the solute is described quantum mechanically.

In previous papers,^{16,18} we have shown that point 1, i.e., the introduction of the MFA, does not introduce significant errors in the calculated properties of water, alcohols, or carbonyl compounds. The same conclusion is reached by Takahashi *et al.*¹⁷ in their study of the water and HO[−] molecules. Therefore, this point does not seem to be at the origin of the discrepancies between the ASEP/MD and DFT/MM/MD

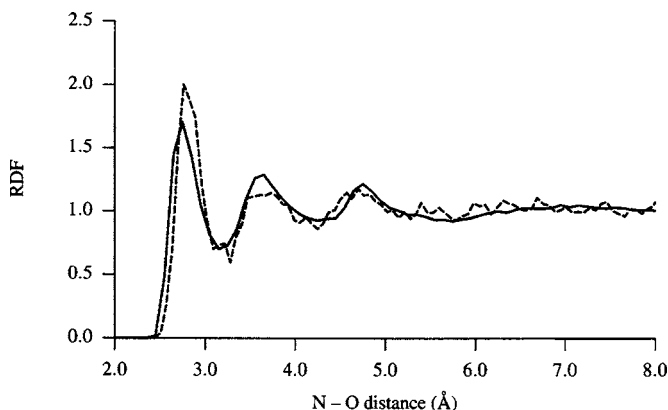


FIG. 6. Comparison between the nitrogen-1 (triazene)-oxygen (water) radial distribution functions obtained with DFMM (dashed line) and ASEP/MD, set 9 (full line).

methods. Furthermore, the error introduced by this approximation in the interaction energy can be estimated using approximate formulas.¹⁶ In the case under study, we estimated that the errors associated with the use of MFA lie between 0.5 and 1.0 kcal/mol.

In order to determine the importance of the second point, the use of fixed versus flexible geometries, we studied the variation of the solute-solvent interaction energy as a function of N–H distance, and N1=N2–N3–H5 and N1=N2–N3–H6 torsion angles. The ASEP/MD simulation assumes fixed geometries, and the iterative procedure can fail if there is a strong correlation between the solute-solvent interaction energy and the internal geometry parameters. To clarify this point, we classified the different solute-solvent configurations obtained in the DFT/MM/MD simulation according to their triazene geometry. In no case did we find a correlation between the interaction energy E_{int} and the N–H distances or torsion angles. Within the tested energy range, E_{int} appeared to be almost independent of the variation of triazene geometric parameters (see Fig. 5). For instance, the average interaction energy calculated for configurations displaying a given N1=N2–N3–H5 angle did not appreciably deviate from the average energy obtained with configurations displaying a different dihedral angle value. Thus, for dihedral angles of 0° and 40°, the average interaction energy difference amounted to 0.5 kcal/mol only.

Finally, we examined the influence of the ASEP solute's point charge distribution type on the simulation results. By default, and following the trend used for most force fields, the ASEP/MD method places a charge on each nucleus of the molecule. Charge values are obtained by fitting the molecular electrostatic potential at points defined either by the CHELPG prescription⁴² or by the position of water molecules in the MD simulation. However, no appreciable differences between the two prescriptions were found in obtaining set 6. To improve the results, the point charge set should therefore include additional charges, in particular to account for lone pairs. In this work, we included one additional charge on each nitrogen atom with sp^2 hybridization, N1 and N2. The charge site lies in the N1N2N3 plane and bisects the H4N1N2 and N1N2N3 angles. N3 requires additional considerations. In vacuo, the N3 is pyramidal, and the lone pair can be well described by one additional charge. In solution, however, N3 is flat, and defining a site for the additional charge is not straightforward. In such a case, the lone pair may be better represented through two charges located one above and one below the molecular plane. Therefore, the following charge sets were tested:

Set 9: One charge on each of the six nuclei, two charges (in the molecular plane) representing the lone pairs of N1 and N2, and one additional charge above the molecular plane representing the N3 lone pair.

Set 10: Same as set 9 but two additional charges are located one above and one below the molecular plane to account for N3 lone pairs.

After some testing, the optimal position for the charges representing the lone pairs was found to be 0.42 Å from the nitrogen atoms. In set 9, the charge representing the N3 lone pair was positioned in such a way that the angles

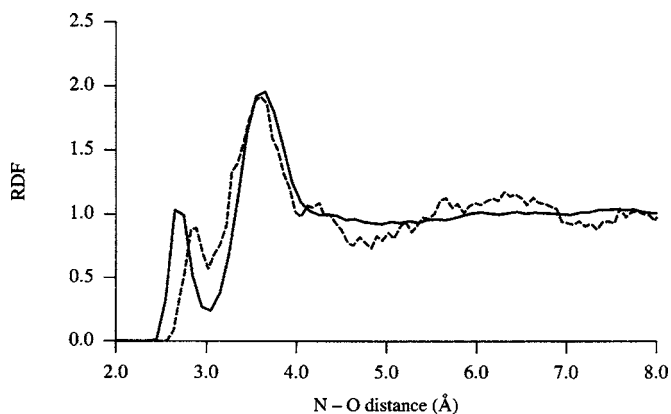


FIG. 7. Comparison between the nitrogen-2 (triazene)-oxygen (water) radial distribution functions obtained with DFMM (dashed line) and ASEP/MD, set 9 (full line).

q -N3–N2, q -N3–H5, and q -N3–H6 (where q is this additional charge) are equal and greater than 90°. For set 10 another charge was placed at the opposite side of N3, i.e., with all the said angles equal but less than 90°. When N3 is planar, the two charges should match and lie on a line perpendicular to the N2–N3–H5–H6 plane and at opposite sides.

The perusal of Table II shows that set 9 and set 10 display the same trend, the dipole moment and the N–H distances increase respect to the set 6 values, becoming, especially with set 10, closer to the DFT/MM/MD values. The most striking improvement provided by the use of these sets concerns the solvent structure around the solute. Figures 6–8 display the N1–O, N2–O, and N3–O rdfs obtained with set 9 (set 10 yields similar results that are not shown for simplicity). The main features of the rdfs present in the DFT/MM/MD simulation, position of the peaks, coordination number (see Table III), etc., are now well reproduced.

Table IV displays the charges on each nuclei and lone pair of the triazene when different point charge sets are used. Obviously, in the case of set 9, the value of the N3 lone pair charge becomes negligible as the molecular geometry approaches planarity so as to preserve the symmetry of the system. Indeed, in our calculations, the triazene molecule becomes almost planar after geometry optimization. Furthermore, given that set 6 already reproduced the solvent struc-

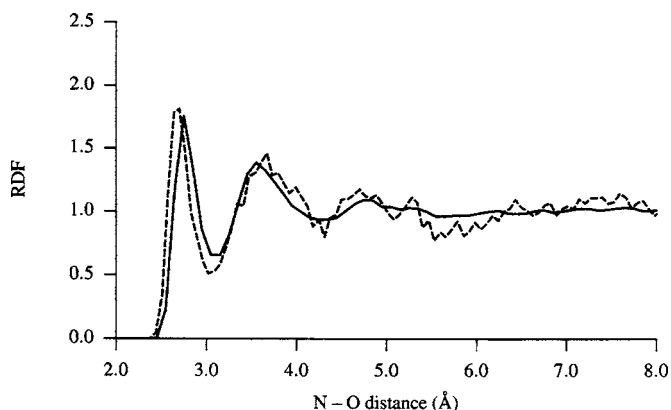


FIG. 8. Comparison between the nitrogen-3 (triazene)-oxygen (water) radial distribution functions obtained with DFMM (dashed line) and ASEP/MD, set 9 (full line).

TABLE III. Coordination numbers of nitrogen atoms of triazene.

| | N1-O | N2-O | N3-O | N1-H | N2-H | N3-H |
|----------------|------|------|------|------|------|------|
| DFT/MM/MD | 2.28 | 0.81 | 1.83 | 1.70 | 0.84 | ... |
| ASEP/MD set 6 | 4.41 | ... | ... | 2.26 | ... | ... |
| ASEP/MD set 9 | 2.41 | 1.02 | 2.11 | 1.62 | 1.00 | ... |
| ASEP/MD set 10 | 2.54 | 1.03 | 2.04 | 1.65 | 1.01 | ... |

ture around N1, that set 9 reproduced adequately the solvent structure around triazene, and that the charge on the lone pair of N3 is negligible, we can conclude that in order to obtain adequate rdfs on N2 and N3 it is compulsory to include a charge on the lone pair of N2. Probably this charge permits the formation of structures such as that displayed in scheme 2 that facilitate the formation of hydrogen bonds on N2 and N3.

Because N3 only forms hydrogen bonds of the type N-H...O, the addition of charges on the lone pair of N3 scarcely improved the description of the solvent structure around this part of the molecule.

Interaction energies

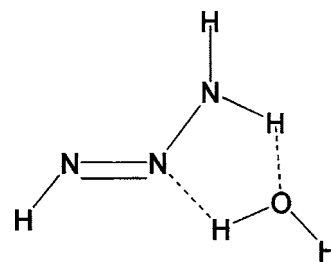
The computed solute-solvent interaction energies are summarized in the last rows of Tables I and II. Although the solute-solvent interaction energy is affected by a large statistical uncertainty that makes comparison difficult, the values computed with set 9 and set 10 are significantly larger and closer to the DFT/MM/MD calculations than the one computed with set 6, clearly showing the importance of the explicit consideration of lone pairs. The differences between the DFT/MM/MD result and those provided by ASEP/MD using set 9 or set 10 are within 7%–10%. Part of the difference can be assigned to small differences in the basis set and to the Stark effect. One may note that the dipole contribution to the Stark effect using the expressions of Ref. 16 yields a value of -0.42 kcal/mol. Given the nature of the molecule under study, one can expect higher multipoles to provide a similar contribution leading to a total Stark effect close to 1 kcal/mol, and reducing the differences with the DFT/MM/MD results to 4%–8%.

It is also interesting to compare the ASEP/MD solute-solvent interaction energy when it is computed in a quantum-classical or classical-classical approach. In the first case, the

solute is represented by its wave function and the solvent through point charges. In the second case, the interaction energy is obtained as in the MD calculation, i.e., using point charges for both the solute and the solvent. In order to make the comparison of these two quantities easier, we added the distortion (polarization) energy of the solute, which is calculated quantum mechanically, to the classical-classical energy. When set 6 is used, the quantum-classical interaction energy is -24.9 kcal/mol and the classical-classical energy is slightly smaller in absolute value, -24.4 kcal/mol. The relative error is therefore rather small, about 2%. When set 9 is used, the corresponding values are -34.2 kcal/mol (quantum-classical) and -36.5 kcal/mol (classical-classical). The error amounts now to 7% (similar results were obtained with set 10). Therefore, the three sets of classical point charges seem to yield a very good estimate of the corresponding quantum-classical energy. However, as stressed above, set 6 yields wrong rdfs and clearly underestimates the DFT/MM/MD solute-solvent interaction energy. The conclusion is that a force field that correctly reproduces the quantum-classical interaction energy for a given solute-solvent configuration does not necessarily lead to a correct solvent structure around the solute and therefore to a correct solute-solvent interaction. The force field must also contain the fundamental physics of the interaction, which in the present case means that some nitrogen lone pairs must be considered explicitly. A final remark can be made. In the values given above, one may notice that the percentage error with set 9 (and set 10) is a little larger than the percentage error with set 6. Set 9 and set 10 correctly predict the existence of solvent molecules hydrogen bonded to N2 and N3, while set 6 does not. Accounting for these hydrogen-bond interactions substantially improves the agreement between the ASEP/MD and DFT/MM/MD interaction energies, although, at the same time, it slightly increases the error of the classical-classical calculation as a consequence of the closer solute-solvent interaction.

TABLE IV. Point charges (in a.u.) on nuclei and lone pairs of triazene in aqueous solution.

| | Set 6 | Set 9 | Set 10 |
|---------------|--------------------|--------------------|--------------------|
| N1 | -0.651 ± 0.006 | -0.258 ± 0.006 | -0.276 ± 0.010 |
| N2 | -0.125 ± 0.006 | 1.102 ± 0.005 | 1.100 ± 0.008 |
| N3 | -0.124 ± 0.004 | -0.710 ± 0.010 | 0.662 ± 0.022 |
| H4 | 0.395 ± 0.002 | 0.338 ± 0.003 | 0.358 ± 0.003 |
| H5 | 0.251 ± 0.002 | 0.447 ± 0.003 | 0.342 ± 0.001 |
| H6 | 0.252 ± 0.004 | 0.414 ± 0.003 | 0.311 ± 0.004 |
| $q_{Lp}(N1)$ | | -0.432 ± 0.005 | -0.446 ± 0.008 |
| $q_{Lp}(N2)$ | | -0.893 ± 0.003 | -0.942 ± 0.007 |
| $q_{1Lp}(N3)$ | | -0.007 ± 0.005 | -0.557 ± 0.013 |
| $q_{2Lp}(N3)$ | | | -0.550 ± 0.005 |



SCHEME 2. Interaction between triazene and water.

CONCLUSIONS

This paper has been devoted to the study of triazene in aqueous solution, as a comparative test case of three solvent models making use of effective Hamiltonians: MPE-continuum, ASEP/MD, and DFT/MM/MD. The main trends run in parallel in the three models, although the continuum approach underestimates the solvent effects on the solute properties, this model improves if a few water molecules are explicitly included into the calculation. Indeed, solvation induces appreciable changes in the geometry and charge distribution of triazene. In water, the molecule adopts an almost planar structure characterized by a high degree of flexibility. Furthermore, the length of the double bond increases and that of the single bond decreases, which may be explained by a greater weight of the zwitterionic form of triazene in solution. The molecule forms about five strong hydrogen bonds with water molecules.

We also analyzed the accuracy of the ASEP/MD method as a function of the solute point charge distribution used in the MD calculation. In order to reproduce the results of QM/MM/MD calculations, the use of explicit point charges representing nitrogen lone pairs in the MD simulation step appears to be compulsory. When this is done, the ASEP/MD results are close to those obtained in the much more computationally demanding DFT/MM/MD calculations. Therefore, the present study validates the use of the mean field approximation provided a physically correct and accurate description of the solute-solvent interaction is used.

ACKNOWLEDGMENTS

This research was sponsored by the Dirección General de Investigación Científica y Técnica (Grant No. CTQ2004-05680) and by the Consejería de Educación y Juventud de la Junta de Extremadura (Grant No.2PR03A071). One of the authors (I.F.G.) thanks the dirección General de Universidades for supporting his stay at Nancy.

¹J. Tomasi and M. Persico, *Chem. Rev.* (Washington, D.C.) **94**, 2027 (1994); C. J. Cramer and D. G. Truhlar, *ibid.* **99**, 2161 (1999); J. Tomasi, B. Mennucci, and R. Cammi, *ibid.* **105**, 2999 (2005).

²J.-L. Rivail and D. Rinaldi, in *Computational Chemistry, Review of Current Trends*, edited by J. Leszczynski (World Scientific, New York, 1996), p. 139.

³D. Rinaldi and J.-L. Rival, *Theor. Chim. Acta* **32**, 57 (1973).

⁴J.-L. Rivail and D. Rinaldi, *Chem. Phys.* **18**, 233 (1976).

⁵V. Dillet, D. Rinaldi, and J.-L. Rivail, *J. Phys. Chem.* **98**, 5034 (1994).

⁶D. Rinaldi, A. Bouchy, J.-L. Rivail, and V. Dillet, *J. Chem. Phys.* **120**, 2343 (2004).

⁷M. L. Sánchez, M. A. Aguilar, and F. J. Olivares del Valle, *J. Comput. Chem.* **18**, 313 (1997).

⁸M. L. Sánchez, M. E. Martín, M. A. Aguilar, and F. J. Olivares del Valle, *Chem. Phys. Lett.* **310**, 195 (1999).

⁹M. L. Sánchez, M. E. Martín, M. A. Aguilar, and F. J. Olivares del Valle, *J. Comput. Chem.* **21**, 705 (2000).

¹⁰M. E. Martín, M. L. Sánchez, F. J. Olivares del Valle, and M. A. Aguilar, *J. Chem. Phys.* **116**, 1613 (2002).

¹¹I. Fdez. Galván, M. E. Martín, and M. A. Aguilar, *J. Comput. Chem.* **25**, 1227 (2004).

¹²I. Tuñón, M. T. C. Martins-Costa, C. Millot, and M. F. Ruiz-López, *J. Mol. Model.* **1**, 196 (1995).

¹³I. Tuñón, M. T. C. Martins-Costa, C. Millot, M. F. Ruiz-López, and J.-L. Rivail, *J. Comput. Chem.* **17**, 19 (1996).

¹⁴I. Tuñón, M. T. C. Martins-Costa, C. Millot, and M. F. Ruiz-López, *J. Chem. Phys.* **106**, 3633 (1997).

¹⁵S. Chalmet and M. F. Ruiz-López, *J. Chem. Phys.* **111**, 1117 (1999).

¹⁶M. L. Sánchez, M. E. Martín, I. Fdez. Galván, F. J. Olivares del Valle, and M. A. Aguilar, *J. Phys. Chem. B* **106**, 4813 (2002).

¹⁷H. Takahashi, S. Takei, T. Hori, and T. Nitta, *J. Mol. Struct.: THEOCHEM* **632**, 185 (2003).

¹⁸M. E. Martín, M. A. Aguilar, S. Chalmet, and M. F. Ruiz-López, *Chem. Phys. Lett.* **344**, 107 (2001).

¹⁹J. C. Scaiano, C. Chen, and P. F. McGarry, *J. Photochem. Photobiol., A* **62**, 75 (1991).

²⁰M. Barra and N. Chen, *J. Org. Chem.* **65**, 5739 (2000).

²¹N. Chen, M. Barra, I. Lee, and N. Chahal, *J. Org. Chem.* **67**, 2271 (2002).

²²J. W. Sutherland, *J. Phys. Chem.* **83**, 789 (1979).

²³R. H. Smith, Jr., C. L. Denlinger, R. Kupper, S. R. Koeple, and C. J. Michejda, *J. Am. Chem. Soc.* **106**, 1056 (1984).

²⁴R. H. Smith, Jr., C. L. Denlinger, R. Kupper, A. F. Mehl, and C. J. Michejda, *J. Am. Chem. Soc.* **108**, 3726 (1986).

²⁵R. H. Smith, B. D. Wladkowski, A. F. Mehl, M. J. Cleveland, E. A. Rudrow, G. N. Chmurny, and C. J. Michejda, *J. Org. Chem.* **54**, 1036 (1989).

²⁶M. N. Ramos and S. R. Pereira, *J. Chem. Soc., Perkin Trans. 2* **1986**, 131.

²⁷A. Schmiedekamp, R. H. Smith, Jr., and C. J. Michejda, *J. Org. Chem.* **53**, 3433 (1988).

²⁸A. Schmiedekamp, I. A. Topol, S. K. Burt, H. Razafinjanahary, H. Chermette, T. Pfaltzgraff, and C. J. Michejda, *J. Comput. Chem.* **15**, 875 (1994).

²⁹P. Charbonneau, B. J. Claude, and M. A. Whitehead, *J. Mol. Struct.: THEOCHEM* **574**, 85 (2001).

³⁰C. C. Pye, K. Vaughan, and J. F. Glister, *Can. J. Chem.* **80**, 447 (2002).

³¹A. D. Becke, *Phys. Rev. A* **38**, 3098 (1988); J. P. Perdew, *Phys. Rev. B* **33**, 8822 (1986).

³²N. Godbout, D. R. Salahub, J. Andzelm, and E. Wimmer, *Can. J. Chem.* **70**, 560 (1992).

³³A. St-Amant and D. R. Salahub, *Chem. Phys. Lett.* **169**, 387 (1990).

³⁴M. J. Frisch, G. W. Trucks, H. B. Schlegel *et al.*, GAUSSIAN 03 (Gaussian, Inc., Wallingford, CT, 2004).

³⁵K. Refson, *Comput. Phys. Commun.* **126**, 310 (2000).

³⁶C. Curutchet, C. J. Cramer, D. G. Truhlar, M. F. Ruiz-López, D. Rinaldi, M. Orozco, and F. J. Luque, *J. Comput. Chem.* **24**, 284 (2003).

³⁷S. Chalmet and M. F. Ruiz-Lopez, *J. Chem. Phys.* **115**, 5220 (2001).

³⁸A. Banerjee, N. Adams, J. Simons, and R. Shepard, *J. Phys. Chem.* **89**, 52 (1985).

³⁹W. L. Jorgensen, J. Chandrasekhar, J. D. Madura, R. W. Impey, and M. L. Klein, *J. Chem. Phys.* **79**, 926 (1983).

⁴⁰W. L. Jorgensen, D. S. Maxwell, and J. Tirado-Rives, *J. Am. Chem. Soc.* **118**, 11225 (1996); W. L. Jorgensen and C. J. Swenson, *ibid.* **107**, 569 (1985).

⁴¹S. Nosé, *Mol. Phys.* **52**, 255 (1984); W. G. Hoover, *Phys. Rev. A* **31**, 1695 (1985).

⁴²C. M. Breneman and K. B. Wiberg, *J. Comput. Chem.* **11**, 361 (1990).